Development 138, 2957-2968 (2011) doi:10.1242/dev.063784

Sprouty genes prevent excessive FGF signalling in multiple cell types throughout development of the cerebellum

Tian Yu[1], Yuichiro Yaguchi[1,2], Diego Echevarria[3], Salvador Martinez[3] and M. Albert Basson[1,4,*]

SUMMARY

Fibroblast growth factors (FGFs) and regulators of the FGF signalling pathway are expressed in several cell types within the cerebellum throughout its development. Although much is known about the function of this pathway during the establishment of the cerebellar territory during early embryogenesis, the role of this pathway during later developmental stages is still poorly understood. Here, we investigated the function of sprouty genes (*Spry1*, *Spry2* and *Spry4*), which encode feedback antagonists of FGF signalling, during cerebellar development in the mouse. Simultaneous deletion of more than one of these genes resulted in a number of defects, including mediolateral expansion of the cerebellar vermis, reduced thickness of the granule cell layer and abnormal foliation. Analysis of cerebellar development revealed that the anterior cerebellar neuroepithelium in the early embryonic cerebellum was expanded and that granule cell proliferation during late embryogenesis and early postnatal development was reduced. We show that the granule cell proliferation deficit correlated with reduced sonic hedgehog (SHH) expression and signalling. A reduction in *Fgfr1* dosage during development rescued these defects, confirming that the abnormalities are due to excess FGF signalling. Our data indicate that sprouty acts both cell autonomously in granule cell precursors and non-cell autonomously to regulate granule cell number. Taken together, our data demonstrate that FGF signalling levels have to be tightly controlled throughout cerebellar development in order to maintain the normal development of multiple cell types.

KEY WORDS: Cerebellum, Sprouty, FGF, SHH, Granule cell, Mouse

INTRODUCTION

The cerebellum is an important control centre for fine motor coordination. The mammalian cerebellum consists of a medial vermis flanked by two hemispheres. Several cell types are found within the cerebellum, including granule cells (GCs, the most numerous type of neuron in the brain) (Hatten and Heintz, 1995), Purkinje neurons (Purkinje cells, PCs), interneurons and Bergmann glia (BG). These cells are organised in layers and folded into characteristic folia. Much is known about the mechanisms responsible for establishing the cerebellar territory in the early embryo; however, the nature of the signalling molecules and regulators required for generating the correct numbers of different types of neurons and glia to establish the complex architecture of the cerebellum is still poorly understood (Hatten and Heintz, 1995; Herrup and Kuemerle, 1997).

The cerebellum is derived from the most anterior segment of the hindbrain, rhombomere 1 (r1). Classical embryological studies in the chick embryo have shown that the isthmic organiser (IsO), located between the mesencephalon (mes) and r1, directs formation of the cerebellum (for a review, see Nakamura et al., 2008). Since the demonstration that fibroblast growth factor 8 (FGF8) can mimic the activity of the IsO in the chick embryo (Crossley et al., 1996; Martinez et al., 1999), a large body of evidence implicating FGF signalling in the survival, specification and patterning of r1 has accumulated (for reviews, see Partanen, 2007; Nakamura et al., 2008). In the mouse, the loss of *Fgf8* expression from the IsO by embryonic day (E) 8.75 is associated with loss of the entire mes and r1 (Chi et al., 2003). Recently, we have shown that embryonic tissues that are located directly adjacent to the IsO (posterior mes and anterior r1) and that are, therefore, exposed to the highest concentration of FGF ligand, are dependent upon these high levels of FGF signalling for development (Basson et al., 2008). Furthermore, deletion of *Fgf8* at later stages of development demonstrated a requirement for prolonged FGF signalling for the normal development of these structures (Sato and Joyner, 2009). The strength or duration of FGF signalling can affect cell fate during mes/r1 development. Ectopic expression of an *Fgf8* splice variant, *Fgf8b*, which encodes an FGF8 isoform with high affinity for FGF receptors (Olsen et al., 2006), in the mouse embryo can induce the expression of markers of r1 and cerebellar fate, such as *Gbx2* (Liu et al., 1999). By contrast, ectopic expression of *Fgf8a*, which encodes an FGF8 isoform with much lower affinity for FGF receptors (Olsen et al., 2006; Zhang et al., 2006), only expands the mes and does not appear to promote cerebellar fate (Lee et al., 1997; Liu et al., 1999).

After establishment of the cerebellar territory from r1, neural progenitors are born in germinal zones and migrate to specific locations within the anlage, where they proliferate and undergo further differentiation and maturation into mature neurons (for reviews, see Hatten and Heintz, 1995; Sotelo, 2004; Zervas et al., 2005; Sillitoe and Joyner, 2007). With the exception of the granule neurons that are derived from the upper rhombic lip (Wingate, 2001; Machold and Fishell, 2005), other classes of neurons and glia are born within the ventricular zone of the cerebellar anlage from ~E11.5 of development. These neuronal precursors migrate radially towards the pial surface on glial fibres. Granule cell precursors (GCps) migrate tangentially over the pial surface of the cerebellum to form the external granular layer (EGL). GCps proliferate

[1]Department of Craniofacial Development, King's College London, London SE1 9RT, UK. [2]Department of Otorhinolaryngology, The Jikei University School of Medicine, Tokyo 105-8461, Japan. [3]Instituto de Neurociencias de Alicante, UMH-CSIC, 03550-San Juan de Alicante, Spain. [4]MRC Centre for Developmental Neurobiology, King's College London, London SE1 1UL, UK.

*Author for correspondence (albert.basson@kcl.ac.uk)

Accepted 4 May 2011

extensively from ~E16.5 through to postnatal day (P) 15 in response to cell surface ligands and secreted growth factors (Dahmane and Ruiz i Altaba, 1999; Wechsler-Reya and Scott, 1999; Klein et al., 2001; Solecki et al., 2001; Corrales et al., 2006) to generate a vast number of granule neurons. Upon cell cycle exit, these cells migrate inwardly on Bergmann glial fibres to form the inner granular layer (IGL) (Sotelo and Changeux, 1974; Hatten et al., 1984; Yacubova and Komuro, 2003).

A key signalling molecule that is required for GCp proliferation is sonic hedgehog (SHH), which is produced by PC precursors (Dahmane and Ruiz i Altaba, 1999; Wallace, 1999; Wechsler-Reya and Scott, 1999; Kenney et al., 2003; Lewis et al., 2004). Exogenous FGF2 has been shown to inhibit the responsiveness of GCps to SHH in vitro and in vivo, resulting in reduced GCp proliferation (Wechsler-Reya and Scott, 1999; Fogarty et al., 2007). Whether endogenous FGF signalling has a direct role in controlling GCp proliferation in vivo remains to be determined. We and others recently reported that many genes encoding FGF ligands and receptors are expressed throughout cerebellar development, including postnatal stages when GCps are proliferating (e.g. Yaguchi et al., 2009). However, with the exception of FGF9, which has been shown to regulate GC migration to the IGL (Lin et al., 2009), no other FGF ligand has been implicated in later stages (>E12.5) of cerebellar development.

Several regulators of embryonic FGF signalling have been identified over the last decade. These include dual specificity phosphatases, Sef (Il17rd – Mouse Genome Informatics), sprouty and spred proteins (Echevarria et al., 2005; Lin et al., 2005; Mason et al., 2006; Bundschu et al., 2007; Li et al., 2007). Sprouty genes encode feedback antagonists of FGF signalling and three Sprouty genes (*Spry1*, *Spry2* and *Spry4*) are expressed in the IsO, posterior mes and anterior r1 (Minowada et al., 1999). We investigated the function of these genes in development of the mouse cerebellum, and found that these genes are required to prevent excessive FGF signalling at multiple stages of cerebellar development. The effects of deregulated signalling on cerebellar morphology depended on the time and cell type in which Sprouty genes were deleted, revealing several distinct functions of these genes during cerebellar morphogenesis.

MATERIALS AND METHODS

Mouse lines

Conditional *loxP*-flanked and null alleles of Sprouty1 (*Spry1*) (Basson et al., 2005), Sprouty2 (*Spry2*) (Shim et al., 2005), Sprouty4 (*Spry4*) (Klein et al., 2006), *Fgfr1* (Xu et al., 2002) have been described. These lines were intercrossed and crossed with the following Cre lines: $En1^{cre/+}$ (Kimmel et al., 2000), *Nestin-Cre* (Tronche et al., 1999) and *Math1-Cre* (Matei et al., 2005) as indicated. All lines were maintained on a mixed genetic background. Tail DNA preparations were genotyped by PCR as described in the original publications. All experimental procedures were approved by the UK Home Office.

Histology, in situ hybridisation and immunohistochemistry

For in situ hybridisation and immunohistochemistry on sections, embryos and brains were dissected in ice-cold PBS, fixed overnight in 4% paraformaldehyde (PFA) and embedded in paraffin wax. Serial sections were cut at 10 μm thickness and dried overnight at 42°C. Some sections were stained with Cresyl Violet for histological analyses. In situ hybridisation was carried out using standard methods. Digoxigenin-labelled antisense probe for *Etv5* (Chen et al., 2005), *Gli1* (Corrales et al., 2004), *Ptch1* (Wechsler-Reya and Scott, 1999), *Shh* (Corrales et al., 2004), *Spry1*, *Spry2* and *Spry4* (Minowada et al., 1999) were used. Immunohistochemistry was carried out with the following primary antibodies: anti-BLBP (Chemicon, AB9558; 1:500), anti-calbindin (Swant, CB-38a; 1:2000), anti-GFAP (Dako, 0334; 1:500), anti-PCP2 (kind gift from Brad Denker, Harvard University, Boston, MA, USA; 1:200), anti-p27 (Santa Cruz; 1:50), anti-S100 (Dako, Z0311; 1:200), anti-BrdU (BD Biosciences, 347580, 1:100; or Abcam, Ab6362, 1:50) and anti-SHH (Developmental Studies Hybridoma Bank, University of Iowa, IA, USA, 5E1; 1:50). Primary antibodies were detected using Alexafluor-conjugated species-specific secondary antibodies (Invitrogen; 1:200) or biotinylated secondary antibodies detected using the Vectastain ABC Kit (Vector Laboratories) and visualised using 0.03% diaminobenzidine (DAB; Sigma).

TUNEL

Cerebella were collected and processed as for immunohistochemistry. TUNEL on paraffin sections was performed by using the In Situ Cell Death Detection Kit Fluorescein (Roche). Sections were dewaxed in xylene and dehydrated through a descending ethanol series to PBS before treating with proteinase K for 15 minutes at 37°C. After washing in PBS for 10 minutes, antigen retrieval was carried out by microwaving sections in 10 mM sodium citrate buffer (pH 6.0) for 2 minutes at low power. Slides were incubated with reaction mix (10% enzyme solution: 90% label solution) at 37°C for 1 hour. After a few washes in PBS in the dark, samples were counterstained with Hoechst 33258.

Whole-mount in situ hybridisation

E9.5 embryos were dissected in ice-cold PBS, fixed overnight in 4% PFA at 4°C and processed for in situ hybridisation as previously described (Wilkinson et al., 1989b). Digoxigenin-labelled antisense probe for *Etv5*, *Gbx2* (Wassarman et al., 1997), *Hoxa2* (Wilkinson et al., 1989a), *Otx2* (Simeone et al., 1993), *Spry1*, *Spry2* and *Spry4* (Minowada et al., 1999) were used.

GCp cell cycle analysis

To quantify the number of cells in S-phase, pregnant females were injected intraperitoneally with 50 mg BrdU (5-bromo-2′-deoxyuridine, Sigma) per kg body weight. Newborn mice up to P10 were injected with 20 mg BrdU per kg body weight. Mice were sacrificed 1 hour later, brains collected and processed as described above. After immunodetection, BrdU labelled and total number of cells in the EGL were counted in 100×100 μm areas (two to three fields in each lobule). The labelling index (LI) was calculated as the BrdU-labelled/total number of GCps. To assess the Q fraction, P4 pups were injected with 20 mg IdU (iododeoxyuridine, Sigma) per kg body weight, followed 2 hours later by six BrdU injections at 3-hourly intervals. Mice were sacrificed 30 minutes after the last injection, sections immunostained for BrdU and IdU (Martynoga et al., 2005) and the Q fraction calculated as described (Takahashi et al., 1993; Takahashi et al., 1996).

Western blot

E18.5 mouse cerebella were dissected in ice-cold PBS and frozen on dry ice immediately. Tissues were washed and homogenised in freshly made 20 mM Tris-HCl (pH 7.3) with a cocktail of protease inhibitors (Roche). Proteins were quantified with BSA Protein Assay Reagent (Pierce). Four cerebella of each genotype were analysed. Total protein (10 μg) was resolved on a NuPAGE 3-8% Tris Acetate gel (Invitrogen) and transferred to a nitrocellulose membrane. The membrane was blocked with 10% goat serum in PBS with 0.25% Tween and incubated with the rabbit anti-Gli3 antibody (Santa Cruz, H-280, sc-20688, 1:100) for an hour at room temperature. After incubating with HRP-conjugated anti-rabbit IgG secondary antibody (1:200, DakoCytomation), signal was detected using ECL Plus detection (GE Healthcare) on an X-ray film (Kodak, BioMax, XAR film, Sigma). Band intensity was scanned and measured using ImageJ.

RESULTS

Sprouty genes are expressed throughout cerebellar development

Previous studies have shown that *Spry1*, *Spry2* and *Spry4* are expressed in and around the IsO at E9.5 and E10.5 (Minowada et al., 1999; Liu et al., 2003). We recently reported that several genes

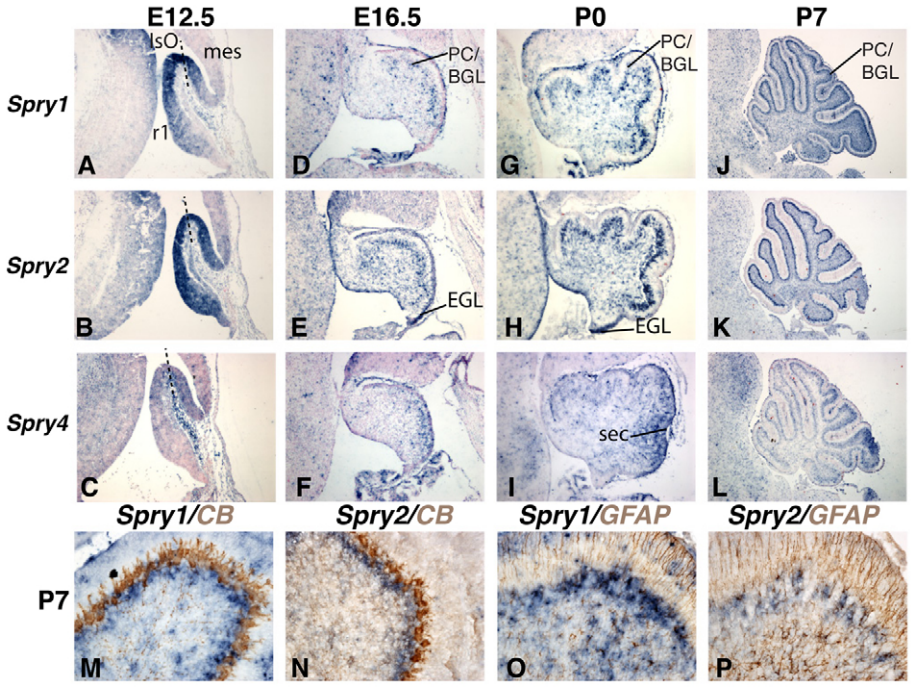

Fig. 1. Sprouty gene expression in the cerebellum during late embryogenesis and early postnatal development. (**A-L**) The expression of *sprouty1* (*Spry1*; A,D,G,J), *sprouty2* (*Spry2*; B,E,H,K) and *sprouty4* (*Spry4*; C,F,I,L) was determined by in situ hybridisation (blue) on sagittal sections of E12.5 (A-C), E16.5 (D-F), P0 (G-I) and P7 (J-L) mouse cerebella, counterstained with Nuclear Fast Red (pink). (**M-P**) P7 cerebellar sections immunostained (brown) with antibodies against calbindin (CB) (M,N) or GFAP (O,P) after in situ hybridisation. Dashed lines in A-C indicate the IsO. EGL, external granular layer; mes, mesencephalon; PC/BGL, Purkinje cell/Bergmann glial cell layer; r1, rhombomere 1; sec, secondary fissure.

encoding FGF ligands, receptors and downstream target genes are expressed in the developing cerebellum after E10.5 (Yaguchi et al., 2009). To determine whether transcripts of sprouty genes are also present during these later stages of cerebellar development, we analysed gene expression by in situ hybridisation at E12.5, E16.5, P0 and P7. *Spry1* and *Spry2* expression were maintained at high levels in the IsO, posterior mes and throughout r1 at E12.5 (Fig. 1A,B). *Spry4* was expressed at low levels (Fig. 1C). At E16.5, all three genes were expressed in the ventricular zone and in cells throughout the cerebellar anlage. Gene expression in the PC/BG cell layer was particularly prominent, and some cells in the EGL and dura were also positive (Fig. 1D-F). *Spry2* transcripts were present at high levels in cells in the posterior EGL (Fig. 1E). By P0, the expression patterns of *Spry1* and *Spry2* were similar to E16.5, with high expression in the PC/BG layer (Fig. 1G,H). *Spry4* expression was low in PC/BG layer and relatively high in GCps around the secondary fissure in the posterior cerebellum (Fig. 1I, sec). At P7, the strongest sprouty gene expression was observed in the PC/BG layer and outer layer of the IGL (Fig. 1J-L). Double immunohistochemistry (IHC) confirmed that most of the sprouty gene expression localised to GFAP+ Bergmann glia underneath the calbindin-positive Purkinje cell layer (PCL; Fig. 1M-P). As sprouty genes are expressed throughout development, we hypothesised that these genes might control several aspects of cerebellar development.

Spry1, *Spry2* and *Spry4* are required for normal cerebellar development

Analysis of $Spry2^{-/-}$ (Shim et al., 2005) mutants revealed that cerebellar development was only mildly affected in these mutants, with a small number of neurons in the most anterior, medial portion of the cerebellar vermis being slightly disorganised (see Fig. S1 in the supplementary material). $Spry1^{-/-}$ (Basson et al., 2005) and $Spry4^{-/-}$ (Klein et al., 2006) cerebella appeared normal (see Fig. S1 in the supplementary material). As a high level of functional redundancy between the sprouty genes during cerebellar development might account for these mild defects, we produced mice lacking more than one sprouty gene (e.g. $Spry1^{-/-};Spry2^{-/-}$). These mice died at birth owing to multi-organ defects (Mahoney Rogers et al., 2011; Taniguchi et al., 2007). To circumvent these lethal defects, we simultaneously deleted two or three conditionally targeted (flanked by *loxP* sites, '*flox*') sprouty alleles specifically from the mes/r1 region of the embryo using an $En1^{cre/+}$ line (Kimmel et al., 2000; Basson et al., 2008) (see Fig. S2 in the supplementary material). These conditional mutants survived to adulthood, which allowed us to determine the functions of sprouty genes during postnatal cerebellar development. Examination of whole brains revealed a change in the overall dimensions of the cerebellar vermis, compared with littermate controls (Fig. 2A). The anteroposterior length of the vermis was reduced in $En1^{cre/+};Spry1^{flox/flox};Spry2^{flox/flox}$ mice, whereas the mediolateral width was increased (Fig. 2B). A mediolateral expansion of the vermis is consistent with our previous findings showing a reduction or loss of vermis tissue when FGF signalling is reduced (Basson et al., 2008). However, the reduction of vermis size in the anteroposterior dimension was unexpected and could not be readily explained by increased FGF signalling from the IsO. Based on previous studies, increased FGF signalling might be predicted to have two possible effects on midbrain development: an enlarged posterior midbrain or fate transformation of midbrain tissue into cerebellum (Crossley et al., 1996; Lee et al., 1997; Liu et al., 1999; Martinez et al., 1999; Nakamura et al., 2008). We found that the posterior midbrain (inferior colliculus, IC) was enlarged in these mutants with no sign of transformation to cerebellum (Fig. 2B). The additional deletion of *Spry4* in $En1^{cre/+};Spry1^{flox/flox};Spry2^{flox/flox};Spry4^{flox/flox}$ animals exacerbated both these defects (Fig. 2C).

Sagittal sections through the cerebellar vermis of these mutants confirmed the marked reduction in size in the anteroposterior dimension, which appeared to be due to thinner GC layers with fewer GCs (Fig. 2D-F). Furthermore, the normal organisation of GCs in smooth folia was also disrupted in these mutants. Neuronal hypocellularity and disorganisation was most severe in the anterior zone of the $En1^{cre/+};Spry1^{flox/flox};Spry2^{flox/flox}$ cerebella, suggesting

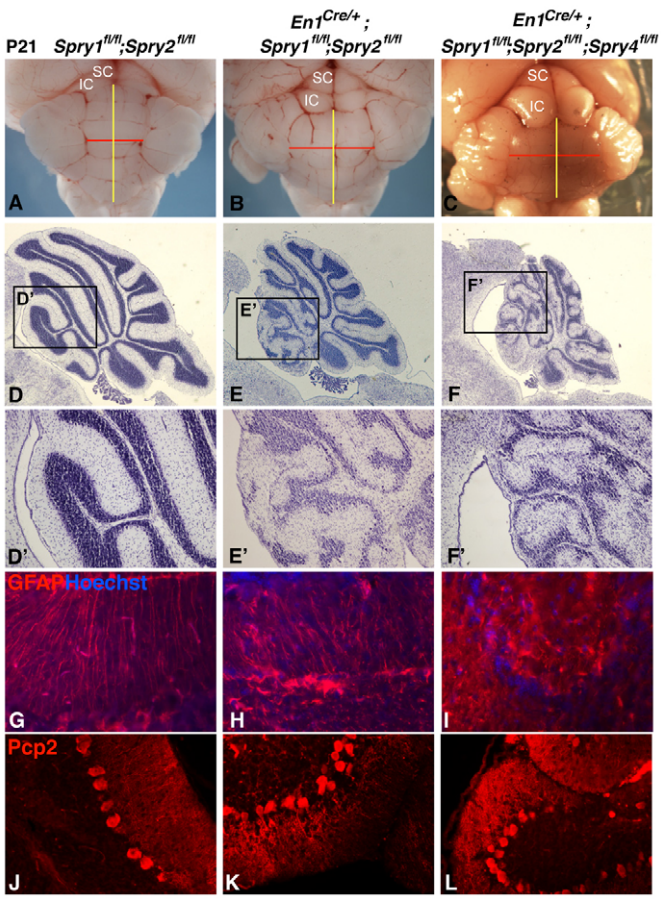

Fig. 2. Sprouty loss of function results in expansion of the vermis and abnormal cytoarchitecture. (**A-C**) Dorsal views of control *Spry1*$^{fl/fl}$;*Spry2*$^{fl/fl}$ (A), *En1*$^{cre/+}$;*Spry1*$^{fl/fl}$;*Spry2*$^{fl/fl}$ (B) and *En1*$^{cre/+}$;*Spry1*$^{fl/fl}$;*Spry2*$^{fl/fl}$;*Spry4*$^{fl/fl}$ (C) whole-mount P21 mouse cerebella. The yellow line indicates the anteroposterior length of the vermis, and the red line indicates the mediolateral width. (**D-F′**) Cresyl Violet-stained sagittal sections of P21 control (D,D′), *En1*$^{cre/+}$;*Spry1*$^{fl/fl}$;*Spry2*$^{fl/fl}$ (E,E′) and *En1*$^{cre/+}$;*Spry1*$^{fl/fl}$;*Spry2*$^{fl/fl}$;*Spry4*$^{fl/fl}$ (F,F′) cerebella; anterior is to the left. D′-F′ are higher magnification views of boxed areas in D-F. (**G-I**) GFAP immunostaining (red) on P21 sagittal sections to detect Bergmann glial fibres, counterstained with Hoechst (blue). High magnification views of the molecular layer are shown. (**J-L**) PCP2 immunostaining (red) on P21 sagittal sections to detect Purkinje cells. IC, inferior colliculus; SC, superior colliculus.

that the anterior zone was more sensitive to deregulated FGF signalling (Fig. 2E,E′). Interestingly, the milder phenotype in the posterior cerebellum was markedly exacerbated by the additional loss of *Spry4* (Fig. 2F). Thus, *En1*$^{cre/+}$;*Spry1*$^{flox/flox}$;*Spry2*$^{flox/flox}$;*Spry4*$^{flox/flox}$ cerebella exhibited severe hypocellularity and disorganisation throughout, indicating that *Spry4*, to a large extent, compensated for the loss of *Spry1* and *Spry2* in the posterior region of *En1*$^{cre/+}$;*Spry1*$^{flox/flox}$;*Spry2*$^{flox/flox}$ cerebella. This ability of *Spry4* to compensate for the loss of the other sprouty genes in the posterior cerebellum is consistent with the higher expression of *Spry4* in this region (Fig. 1F,I,L). Immunostaining for GFAP and calbindin to visualise Bergmann glia and PCs, respectively, revealed abnormalities in these cells. Regularly spaced, thin Bergmann glial processes that are perpendicular to the pial surface normally span the molecular layer (Fig. 2G). In sprouty mutants, glial processes appeared thicker and disorganised (Fig. 2H,I). PCs are large neurons organised in a monolayer between the molecular and GC layers with elaborate dendritic trees extending into the molecular layer (Fig. 2J). PC soma appeared smaller and disorganised in sprouty mutants (Fig. 2K,L). We concluded that *Spry1*, *Spry2* and *Spry4* were essential for the normal morphogenesis and cytoarchitecture of the cerebellum. All three of these genes appear to perform largely overlapping roles, as no unique function could be ascribed to an individual gene and all sprouty-deficient phenotypes were enhanced by a further reduction in sprouty gene dosage.

Sprouty genes function as FGF antagonists in the IsO

Our data thus far indicated that sprouty genes were expressed throughout cerebellar development and that several cell types required sprouty gene function for their normal development. The next step was to identify the exact developmental defects caused by sprouty gene loss of function. Before focusing on the development of particular cell types, we first asked whether sprouty genes functioned as FGF antagonists in the context of the embryonic IsO. To determine whether FGF signalling in mes/r1 cells was affected by the loss of sprouty genes, we analysed the expression of genes transcriptionally regulated by FGF signalling. *Etv5* (*Erm*) is expressed in the IsO and in cells in the posterior mes and anterior r1 flanking the IsO (Fig. 3A). *Etv5* expression was significantly upregulated and expanded around the IsO of *En1*$^{cre/+}$;*Spry1*$^{flox/flox}$;*Spry2*$^{flox/flox}$ embryos (Fig. 3B). *Etv5* expression was further increased and expanded in *En1*$^{cre/+}$;*Spry1*$^{flox/flox}$;*Spry2*$^{flox/flox}$;*Spry4*$^{flox/flox}$ embryos (Fig. 3C), suggesting that all three sprouty genes functioned redundantly as FGF antagonists in mes/r1. Next, we tested whether increased FGF signalling affected gene expression patterns in the mes/r1 region. Exogenous FGF8b has been shown to promote cerebellar fate by inducing the expression of the r1 marker *Gbx2* (Hidalgo-Sanchez et al., 1999; Liu et al., 1999). *Gbx2* expression was increased and expanded in sprouty mutant embryos (Fig. 3D-F), consistent with a previous study (Lin et al., 2005). FGF signals can also repress the mesencephalic marker *Otx2* and GBX2 and OTX2 mutually repress each other's expression (Joyner et al., 2000). Compared with control embryos in which *Gbx2* and *Otx2* gene expression sharply abuts at the IsO (Fig. 3D,G), *Gbx2* expression appeared to be expanded anteriorly and *Otx2* expression appeared to be repressed in a complementary pattern in sprouty mutant embryos (Fig. 3E,F,H,I). Using *Hoxa2* expression as a marker of the posterior border of r1 in combination with *Otx2* to indicate the anterior limit of r1 (Fig. 3G), we confirmed that r1 was significantly expanded in sprouty mutant embryos (Fig. 3H,I). Interestingly, this expansion of r1 tissue correlated well with the enlarged *Gbx2* expression domain in anterior r1, suggesting that the expansion of r1 was due to an increase in the size of anterior r1, the region immediately adjacent to the source of FGF signalling.

Genetic inducible fate mapping studies have shown that the anterior portion of r1 (marked here by high *Gbx2* expression) is fated to become the cerebellar vermis (Sgaier et al., 2005). Thus, the expansion of the *Gbx2* positive anterior r1 in sprouty mutant embryos provided an explanation for the enlarged vermis along the mediolateral plane that characterised these mutant cerebella by P21 (Fig. 2A-C).

Increased FGF signalling in the vicinity of the IsO during early embryogenesis could not readily explain the other defects observed in the sprouty-deficient cerebella. To determine which of these

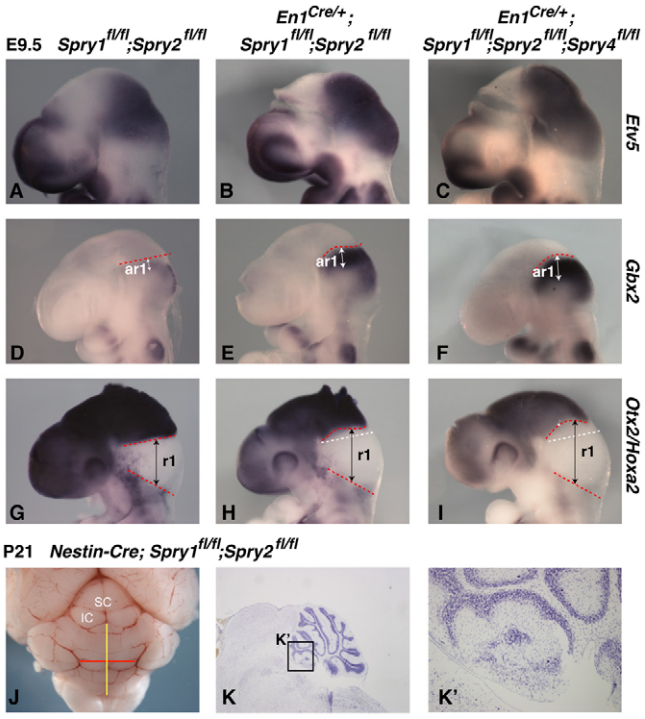

Fig. 3. Sprouty genes function as negative regulators of FGF signalling at the IsO in the early embryo, whereafter they are required for the normal production of granule neurons. (**A-I**) Whole-mount in situ hybridisation of *Etv5* (A-C), *Gbx2* (D-F) and *Otx2;Hoxa2* (G-I) on E9.5 control (*Spry1*$^{fl/fl}$;*Spry2*$^{fl/fl}$; A,D,G); *En1*$^{cre/+}$;*Spry1*$^{fl/fl}$;*Spry2*$^{fl/fl}$ (B,E,H) and *En1*$^{cre/+}$;*Spry1*$^{fl/fl}$;*Spry2*$^{fl/fl}$;*Spry4*$^{fl/fl}$ (C,F,I) mouse embryos. Red dashed lines in D-F indicate the anterior limit of *Gbx2* expression and white arrows the approximate size of anterior r1 (ar1) as marked by *Gbx2*. Red dashed lines in G-I mark the anterior and posterior limits of r1 as indicated by *Otx2* and *Hoxa2*, respectively, and black arrows the approximate size of r1. The white dashed lines in H and I indicate the approximate position of the *Gbx2* expression limit in the control embryo for comparison. (**J**) Dorsal view of a whole-mount *Nestin-Cre;Spry1*$^{fl/fl}$;*Spry2*$^{fl/fl}$ cerebellum at P21. (**K**,**K′**) Cresyl Violet-stained sagittal sections from the brain shown in J. K′ is a higher magnification view of the boxed area in K. IC, inferior colliculus; SC, superior colliculus.

defects were due to the absence of sprouty gene function after E9.5, we produced conditional mutants in which sprouty genes were deleted in all neural and glial progenitors between E10 and E11 of development using a *Nestin-Cre* line (see Fig. S2 in the supplementary material). *Nestin-Cre;Spry1*$^{flox/flox}$;*Spry2*$^{flox/flox}$ mutant cerebella exhibited a thinner GC layer, abnormal foliation and disorganised neurons and glia, indicating that these defects were not secondary to abnormalities during r1 specification in the early (E9.5) embryo (Fig. 3J-K′).

As deletion of two or three sprouty genes in mes/r1 resulted in qualitatively similar phenotypes, we continued our analyses of cerebellar development in *En1*$^{cre/+}$;*Spry1*$^{flox/flox}$;*Spry2*$^{flox/flox}$ mutants to minimise the numbers of animals used in our experiments.

Sprouty genes are required to maintain a self-renewing GCp population and prevent their premature differentiation

Sprouty mutant cerebella are characterised by reduced thickness of the GC layer, suggesting that the production of granule neurons was reduced during development. To determine whether the generation of GC precursors from the rhombic lip was compromised, we visualised these cells shortly after their production was initiated (Machold and Fishell, 2005). At E13.5, the cerebellar anlage of sprouty mutant embryos appeared slightly larger than control littermates, in agreement with the expansion of r1 observed at E9.5 (Fig. 3H,I). No difference in the number or distribution of *Math1* (*Atoh1* – Mouse Genome Informatics)+ cells was observed in sprouty mutants at E13.5, excluding a major defect in the specification or production of these cells from the rhombic lip (Fig. 4A,B). Furthermore, *Math1*+ cells were present along the whole pial surface of the cerebellar anlage, up to its most anterior edge, excluding any abnormalities in tangential migration. By E16.5, when GCps in the EGL had started proliferating, the EGL appeared slightly thinner in the anterior zone of mutant cerebella (Fig. 4C,D). The analysis of developing cerebella at birth (P0) revealed that foliation was initiated as normal with all fissures present. However, some fissures were more shallow and the EGL appeared thinner in the mutants. In addition, the EGL appeared to be completely absent in some areas, especially at the base of some of the forming fissures in the anterior zone (Fig. 4E,F). By P7, the mutant cerebella were smaller and the EGL was thinner than that of control littermates (Fig. 4G,H). Mutant granule cells were disorganised, especially in the anterior region. Furthermore, small regions could be observed where the EGL was almost absent, presumably owing to the loss of GCps (inset in Fig. 4G,H).

These data suggested that the reduction in GC numbers was not due to defects in the formation or migration of GCps from the rhombic lip, but rather due to a failure to maintain the rapidly dividing population of GCps in the EGL from E16.5 onwards. To find evidence for this, we first quantified the number of proliferating GCps at P0, when the first clear evidence of abnormalities in the EGL emerged in the sprouty mutants. The fraction of proliferating progenitors that incorporated BrdU was significantly reduced throughout the mutant cerebella (Fig. 4I-K). To determine whether the failure to maintain sufficient numbers of proliferating progenitors was associated with enhanced GCp differentiation, we stained sections for TAG1 (CNTN2 – Mouse Genome Informatics), an early differentiation marker of cells in the EGL (Bizzoca et al., 2003), and p27^{Kip1} (p27; CDKN1B – Mouse Genome Informatics), a cyclin-dependent protein kinase inhibitor, which is present at high levels in postmitotic GCps in the inner EGL (Miyazawa et al., 2000). Consistent with previous reports, TAG1-expressing pre-migratory cells in the inner EGL represented approximately one-third of the total EGL in control cerebella (Fig. 4L). By contrast, the inner EGL corresponded to approximately half of the EGL in sprouty mutant cerebella (Fig. 4M). Furthermore, the number of cells in the inner EGL with high levels of p27 appeared to be increased in mutant cerebella compared with controls, and p27-positive cells were also detected in the outer EGL in sprouty mutant cerebella (Fig. 4N,O). To quantify cell differentiation within a specific time window, we labelled proliferating cells by injecting pups with the thymidine analogue IdU, followed 2 hours later by the cumulative labelling of proliferating cells by five BrdU injections at 3 hourly intervals. The fraction (Q) of IdU-labelled cells that exited the cell cycle and differentiated without incorporating BrdU, relative to IdU-labelled cells that continued cycling and therefore incorporated BrdU during the 17.5-hour period was calculated (Takahashi et al., 1993; Takahashi et al., 1996). In control cerebella, ~5-10% of GCps stopped cycling and differentiated during a 17.5-hour window (Q fraction=0.05-0.1; Fig. 4P,R). By contrast, 11-22% of GCps exited the cell cycle and differentiated in sprouty mutants (Q fraction=0.11-0.22; Fig. 4Q,R). We concluded that the reduced number of GCs and

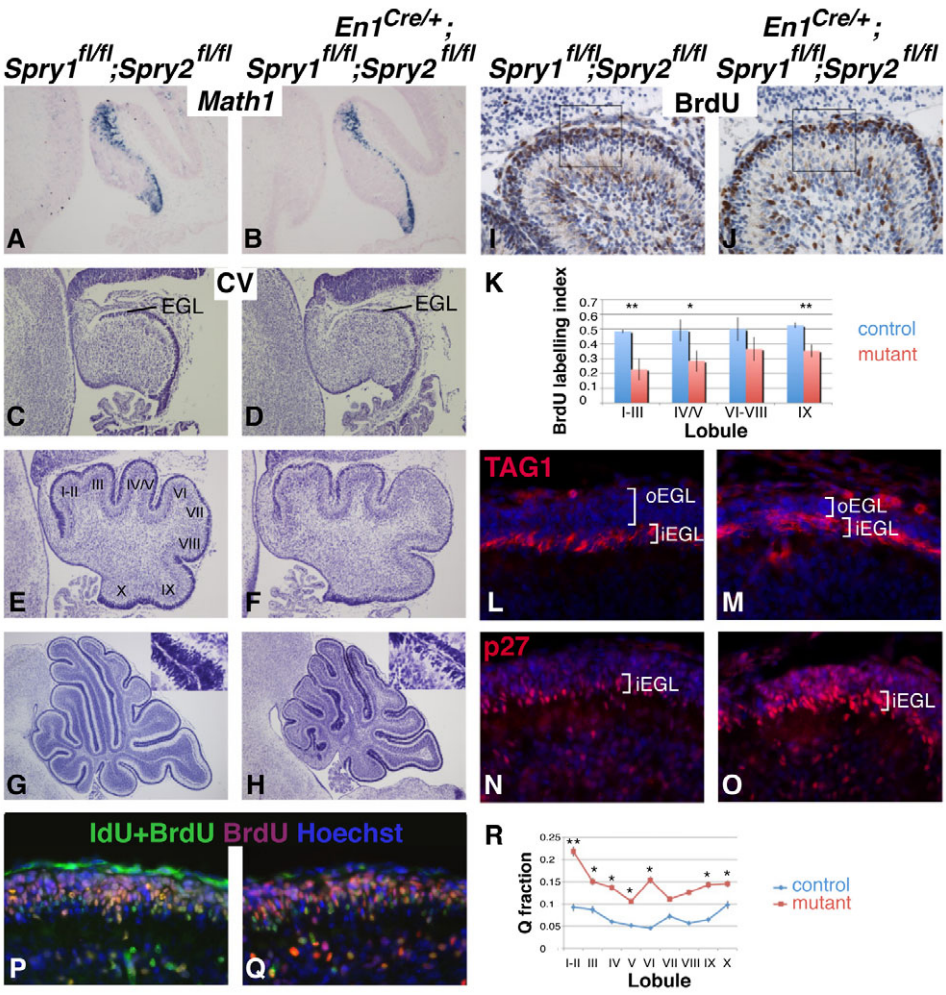

Fig. 4. Reduced proliferation and enhanced differentiation of GCps in sprouty mutants. (**A**,**B**) The presence of *Math1*+ GCps as visualised in sagittal sections from E13.5 control (*Spry1*$^{fl/fl}$;*Spry2*$^{fl/fl}$) and *En1*$^{cre/+}$;*Spry1*$^{fl/fl}$;*Spry2*$^{fl/fl}$ mouse cerebella by in situ hybridisation. (**C-H**) Cresyl Violet (CV) staining of E16.5 (C,D), P0 (E,F) and P7 (G,H) control and mutant sagittal sections. Insets in G and H are high magnification views of the external granular layer (EGL). (**I**,**J**) Sagittal sections through P0 cerebella from control and mutant animals treated with BrdU and immunostained with an antibody against BrdU (brown), counterstained with Haematoxylin. BrdU-positive GCps and total GCps in the EGL were counted in 100×100 μm areas as indicated by the boxes and used to calculate the BrdU labelling index. (**K**) Comparison of BrdU labelling indices in different lobules at P0. Note the significantly reduced labelling indices in mutants (red bar) compared with controls (blue bar) (*P<0.05, **P<0.001, Student's t-test, n=4 per genotype). Error bars represent s.e.m. (**L**,**M**) TAG1 immunohistochemistry (red) to mark the inner EGL (iEGL), counterstained with Hoechst (blue) to visualise the outer EGL (oEGL). Note the alteration in relative thickness of the oEGL and iEGL (white brackets). (**N**,**O**) p27 immunohistochemistry (red) to visualise cells that are exiting the cell cycle and initiation differentiation. (**P**,**Q**) Sagittal sections of P4.5 control and mutant brains after BrdU and IdU injections as described in Materials and methods, immunostained with monoclonal antibodies against both BrdU and IdU (green), BrdU alone (red), and counterstained with Hoechst (blue). (**R**) Q fractions in different lobules (I-X) from control (blue) and mutant (red) cerebella. Note the increased cell cycle exit (differentiation) in mutants compared with controls (*P<0.05, **P<0.001, Student's t-test, n=3 per genotype).

thinner GC layers in the mutant cerebella at P21 were due to fewer GCps in the postnatal EGL being maintained in a proliferative, undifferentiated state.

To exclude the possibility that cell death was responsible for reduced granule cell numbers, apoptotic cells were identified by TUNEL at E18.5, P0 and P3. No differences were detected between the mutants and littermate controls (see Fig. S3 in the supplementary material).

Cerebellar defects in sprouty mutant animals are caused by increased FGF and reduced SHH signalling

Having established that sprouty genes are required for normal levels of GCp proliferation in the postnatal cerebellum, we wanted to understand how loss of sprouty function resulted in this defect. As the SHH pathway has been implicated in GCp proliferation and exogenous FGF2 has been shown to inhibit the responsiveness of GCps to SHH (Wechsler-Reya and Scott, 1999; Fogarty et al., 2007), we tested whether these signalling pathways were deregulated in the early postnatal cerebellum. As expected, the expression of genes positively regulated by FGF signalling, *Etv4* (*Pea3*) (not shown) and *Etv5* (*Erm*), were upregulated in the postnatal cerebellum, confirming that sprouty genes also functioned as FGF antagonists at this stage of development (Fig. 5A,B). The expression of *Gli1* and *Ptch1*, transcriptional targets of SHH signalling in the cerebellum (Corrales et al., 2004), was downregulated (Fig. 5C-F), consistent with a model whereby SHH signalling was inhibited by excessive FGF signalling (Wechsler-Reya and Scott, 1999).

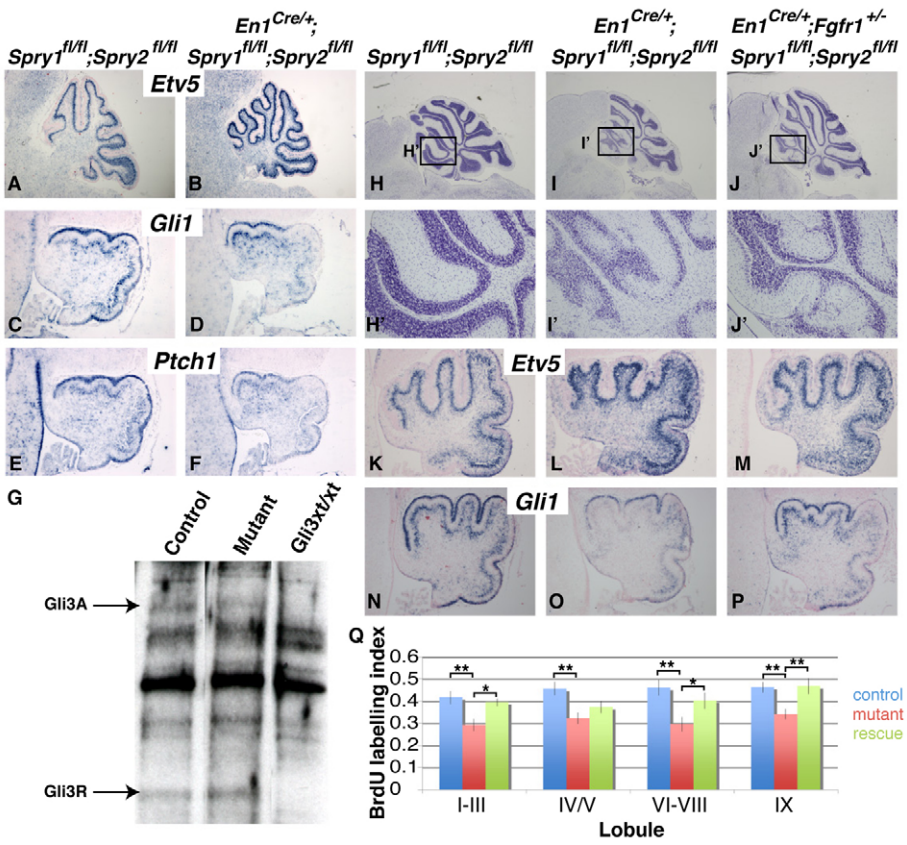

Fig. 5. Increased FGF signalling in sprouty mutant cerebella is associated with reduced SHH signalling and reduced GCp proliferation. (**A-F**) The expression of *Etv5* at P6 (A,B), *Gli1* (C,D) and *Ptch1* (E,F) at E18.5 in control (*Spry1*$^{fl/fl}$;*Spry2*$^{fl/fl}$) and *En1*$^{cre/+}$;*Spry1*$^{fl/fl}$;*Spry2*$^{fl/fl}$ mutant mouse cerebella was determined by in situ hybridisation; sagittal sections are shown, anterior to the left. (**G**) GLI3 western blot from total cell lysates prepared from E18.5 cerebella. Control=*Spry1*$^{fl/fl}$;*Spry2*$^{fl/fl}$, Mutant=*En1*$^{cre/+}$;*Spry1*$^{fl/fl}$;*Spry2*$^{fl/fl}$. Note the absence of GLI3 protein in homozygous *Gli3*$^{xt/xt}$ (Gli3xt/xt) mutant cerebellum (Schimmang et al., 1992). (**H-J′**) Sagittal sections from P21 control, *En1*$^{cre/+}$;*Spry1*$^{fl/fl}$;*Spry2*$^{fl/fl}$ and *En1*$^{cre/+}$;*Spry1*$^{fl/fl}$;*Spry2*$^{fl/fl}$;*Fgfr1*$^{+/-}$ mutants stained with Cresyl Violet. H′,I′ and J′ are high magnification views of the boxed areas in H,I and J, respectively. (**K-P**) The expression of *Etv5* (K-M) and *Gli1* (N-P) on sagittal sections from newborn control, *En1*$^{cre/+}$;*Spry1*$^{fl/fl}$;*Spry2*$^{fl/fl}$ and *En1*$^{cre/+}$;*Spry1*$^{fl/fl}$;*Spry2*$^{fl/fl}$;*Fgfr1*$^{+/-}$ cerebella. (**Q**) BrdU labelling index comparison between P0 control (blue), *En1*$^{cre/+}$;*Spry1*$^{fl/fl}$;*Spry2*$^{fl/fl}$ mutant (red) and *En1*$^{cre/+}$;*Spry1*$^{fl/fl}$;*Spry2*$^{fl/fl}$;*Fgfr1*$^{+/-}$ rescue (green) cerebella. Note significant differences (*P<0.05, **P<0.001, one-way ANOVA, n=4 per genotype) between control and mutants in all lobules, and between mutant and rescue samples in all lobules apart from IV/V. Error bars represent s.e.m.

As an additional read-out of SHH signalling, we quantified the post-translational processing of GLI3. GLI3 exists in the cell as either a full-length protein (190 kDa), which acts as a transcriptional activator of genes regulated by SHH signalling, or a cleaved 80 kDa form, which acts as a repressor. SHH signalling inhibits this processing of the full-length protein (Wang et al., 2000). We measured the ratio between the full-length GLI3 (GLI3A) and the cleaved isoform (GLI3R) (Fig. 5G). At E18.5, the ratio of GLI3A:GLI3R was 0.87±0.04 in control cerebella (n=4), compared with sprouty mutants, in which this ratio was significantly decreased to 0.71±0.04 (P<0.05). This observation further supports our conclusion that SHH signalling is downregulated in sprouty-deficient cerebella.

To prove that the reduced SHH signalling was caused by excessive FGF signalling and that increased FGF signalling was indeed responsible for the observed phenotypes in sprouty-deficient cerebella, we reduced FGF signalling during development. To achieve this, the dosage of the FGF receptor 1 gene, which encodes a high affinity FGF receptor expressed throughout cerebellar development (Trokovic et al., 2003), was reduced. *Fgfr1*$^{+/-}$ mice were normal, indicating that halving the *Fgfr1* gene dosage is not sufficient to disrupt normal development (data not shown). At P21, *En1*$^{cre/+}$;*Spry1*$^{flox/flox}$;*Spry2*$^{flox/flox}$;*Fgfr1*$^{+/-}$ cerebella (n=4) exhibited a striking rescue of the sprouty phenotype (Fig. 5H-J′). Although the granule cell layers (GCLs) were still slightly thinner compared with normal controls, the cerebella were of normal size and neuronal disorganisation was restricted to the most anterior portion of the cerebellum (lobule I, Fig. 5J′). The phenotypic rescue correlated with a rescue of excessive FGF signalling (Fig. 5K-M) as well as a rescue of the reduced SHH signalling in the early postnatal cerebellum (Fig. 5N-P). The latter observation demonstrated that increased FGF signalling was responsible for the reduced SHH signalling in the developing cerebellum, in agreement with previous studies where exogenous FGF was shown to inhibit SHH signalling and GCp proliferation (Wechsler-Reya and Scott, 1999; Fogarty et al., 2007). To confirm that the normalisation of FGF and SHH signalling levels in *En1*$^{cre/+}$;*Spry1*$^{flox/flox}$;*Spry2*$^{flox/flox}$; *Fgfr1*$^{+/-}$ cerebella was indeed associated with a rescue of GCp proliferation levels, proliferating cells were labelled by BrdU in newborn (P0) brains. GCp proliferation was increased in these

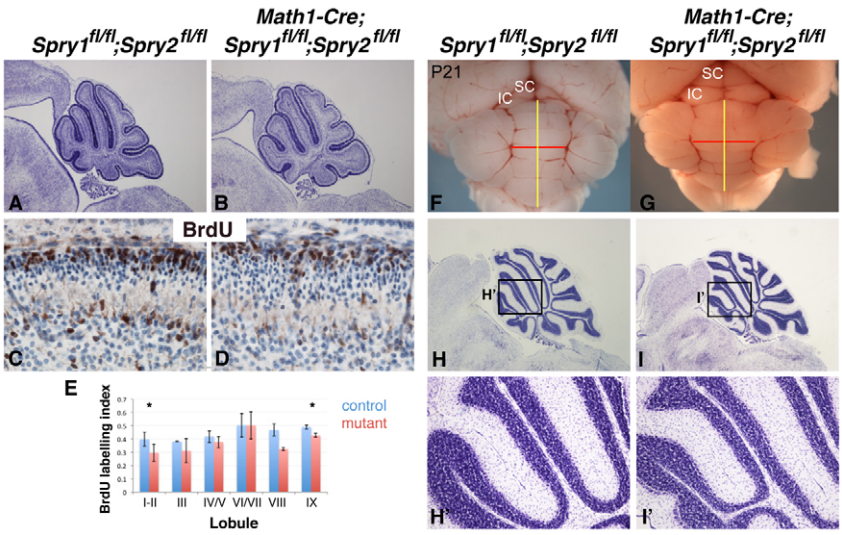

Fig. 6. Sprouty gene deletion in granule cell precursors has a minor effect on cell proliferation. (**A**,**B**) Cresyl Violet staining of sagittal sections through P3 control (*Spry1*$^{fl/fl}$;*Spry2*$^{fl/fl}$) and *Math1-Cre;Spry1*$^{fl/fl}$;*Spry2*$^{fl/fl}$ mouse cerebella. (**C**,**D**) BrdU immunostaining (brown) on sagittal sections counterstained with Hematoxylin (blue). (**E**) BrdU labelling indices at P3 show a minor reduction in proliferation in the anterior and posterior lobules of the mutant cerebella (**P*<0.05, Student's *t*-test, *n*=3 per genotype). Error bars represent s.e.m. (**F-I′**) Whole-mount views (F,G) of and Cresyl Violet-stained sagittal sections (H-I′) through P21 control (*Spry1*$^{fl/fl}$;*Spry2*$^{fl/fl}$) and *Math1-Cre;Spry1*$^{fl/fl}$;*Spry2*$^{fl/fl}$ cerebella. H′ and I′ are higher magnification views of the boxed areas in H and I, respectively. IC, inferior colliculus; SC, superior colliculus.

Fgfr1$^{+/-}$ mutants (rescue) such that the BrdU labelling indices were statistically different from those in the corresponding regions of mutant cerebella, with the exception of lobules IV/V (Fig. 5Q).

To test whether sprouty genes function cell-autonomously within GCps to maintain them in a proliferative state, we deleted these genes specifically in GCps using a *Math1-Cre* transgene (Schuller et al., 2007) (see Fig. S2 in the supplementary material). The EGL in *Math1-Cre;Spry1*$^{flox/flox}$;*Spry2*$^{flox/flox}$ cerebella appeared only slightly thinner at P3 (Fig. 6A-D) and foliation and neuronal organisation appeared normal (Fig. 6A,B). GCp proliferation was reduced in the postnatal EGL of *Math1-Cre;Spry1*$^{flox/flox}$;*Spry2*$^{flox/flox}$ animals (Fig. 6C-E). However, this reduction in GCp proliferation was less pronounced than in the *En1*$^{cre/+}$;*Spry1*$^{flox/flox}$;*Spry2*$^{flox/flox}$ mutants and only significant in the anterior (I-II) and posterior (IX) lobules. These data suggest that sprouty genes can regulate GCp proliferation cell-autonomously, albeit to a limited degree. Analysis of *Math1-Cre;Spry1*$^{flox/flox}$;*Spry2*$^{flox/flox}$ cerebella at P21 confirmed that the effects of deleting sprouty genes in GCps could not fully recapitulate the phenotype observed in the *En1*$^{cre/+}$;*Spry1*$^{flox/flox}$;*Spry2*$^{flox/flox}$ mutants (Fig. 6F-I′). The observation that the loss of sprouty genes in GCps could not fully account for the GC phenotype in the *En1*$^{cre/+}$;*Spry1*$^{flox/flox}$;*Spry2*$^{flox/flox}$ mutants is consistent with their low expression levels in this cell type (Fig. 1). We therefore sought to analyse the development of other cell types that could contribute to this phenotype.

Abnormal differentiation of Bergmann glia and PCs in sprouty mutants

Sprouty genes are expressed at high levels in Bergmann glia and these cells exhibit structural abnormalities by P21 (Fig. 2G-I). To identify the origin of these defects, we followed their development during embryogenesis. The first sign of differentiated Bergmann glia in the cerebellar anlage was the appearance of brain lipid binding protein (BLBP)+ glial fibres in the dorsal-anterior region of the cerebellar anlage (Fig. 7A,A′). It was difficult to detect the presence of BLBP+ radial glia in the mutants at this stage, suggesting that the differentiation of these cells is affected by the loss of sprouty genes (Fig. 7B,B′). By E14.5, a small population of BLBP+ glial cells could be observed in the anterior-dorsal region, extending glial fibres from their cell bodies out to the pial surface where they contacted the basement membrane in so-called 'end feet' structures (Fig. 7C). Glial fibres in the sprouty mutant cerebella appeared twisted and shorter and no clear organisation was evident (Fig. 7D). By P0, most BG cell bodies (positive for S100) were present in the BG/PCL in normal cerebella (area between dotted white lines in Fig. 7E), whereas many S100+ cells were found in ectopic positions in the molecular layer of the mutants (white arrowheads in Fig. 7F). By P7, disorganised, abnormally thick GFAP+ glial fibres could be observed in the mutant cerebella (Fig. 7G,H).

A similar analysis of PC differentiation indicated that PC precursors developed normally during embryogenesis and that these cells were normally distributed in newborn cerebella (Fig. 7I-J′). However, by P7, the PCs in mutant cerebella failed to organise in monolayers and extend dendritic arborisations as they do in controls (Fig. 7K,L). As this defect in PC differentiation appeared late in development, i.e. after BG and GCp defects became evident, and sprouty gene expression in these cells was extremely low (Fig. 1), we concluded that these structural PC defects were most likely to be secondary to defects in BG and GCps.

Sprouty genes are required to maintain normal levels of SHH expression in the postnatal cerebellum

As the cell type-specific deletion of sprouty genes from GCps only had a small effect on GCp proliferation, modulation of GCp responsiveness to SHH could not fully explain the reduction in GCp proliferation in *En1*$^{cre/+}$;*Spry1*$^{flox/flox}$;*Spry2*$^{flox/flox}$ cerebella. Thus, we considered the possibility that defects in the other cell types affected by the loss of sprouty genes, PCs and Bergmann glia might contribute to this phenotype. As PCs appear to be the major source of SHH in the developing cerebellum (Lewis et al., 2004), we considered the possibility that SHH production was abnormal in sprouty mutants. Indeed, fewer PCs expressed *Shh* and the overall levels of *Shh* expression appeared to be reduced in *En1*$^{cre/+}$;*Spry1*$^{flox/flox}$;*Spry2*$^{flox/flox}$ cerebella by E18.5 (Fig. 8A-B′). Immunohistochemical detection of SHH protein at P4 confirmed the absence of PCs with high SHH protein levels (Fig. 8C,D). As SHH is required for normal PC differentiation, this observation might also explain the postnatal PC defects (Dahmane and Ruiz i Altaba, 1999). To test whether reduced *Shh* expression was also

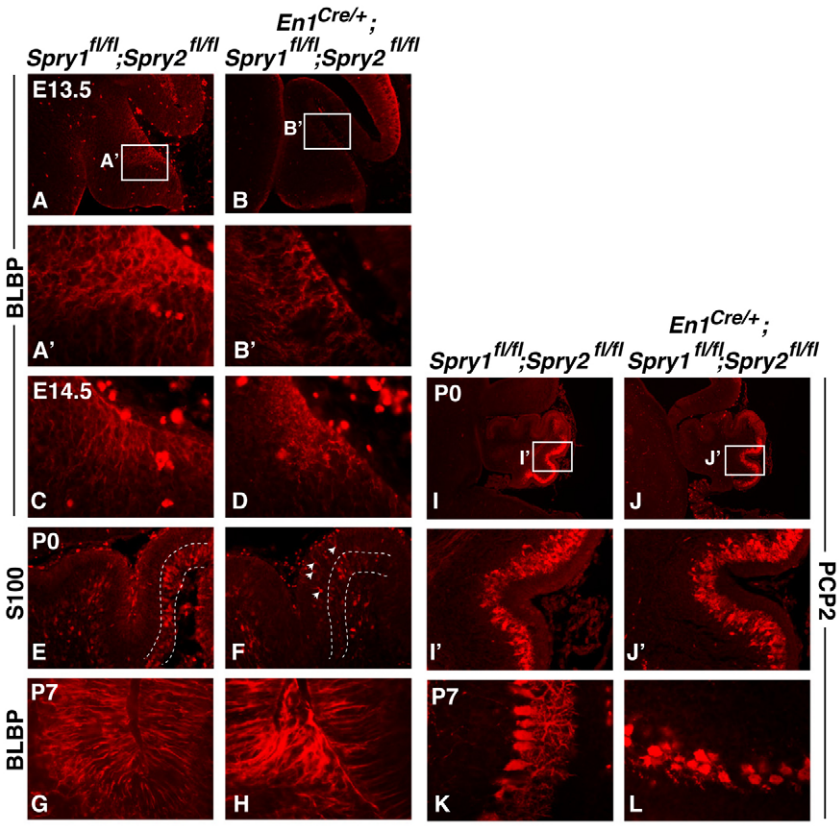

Fig. 7. Sprouty gene function is required for the normal differentiation of Bergmann glia and Purkinje cells. (**A-H**) Sagittal sections of E13.5 (A-B′), E14.5 (C,D), P0 (E,F) and P7 (G,H) control (*Spry1*$^{fl/fl}$;*Spry2*$^{fl/fl}$) and *En1*$^{cre/+}$;*Spry1*$^{fl/fl}$;*Spry2*$^{fl/fl}$ mouse cerebella immunostained with anti-BLBP (A-D,G,H) or S100 (E,F) antibodies. A′ and B′ are high magnification views of the boxed areas in A and B, respectively. Area outlined in E and F is the PC/BG cell layer. (**I-L**) Sagittal sections of P0 (I-J′) and P7 (K,L) control (*Spry1*$^{fl/fl}$;*Spry2*$^{fl/fl}$) and *En1*$^{cre/+}$;*Spry1*$^{fl/fl}$;*Spry2*$^{fl/fl}$ cerebella immunostained with anti-PCP2 antiserum. I′ and J′ are high magnification views of the boxed areas in I and J, respectively.

caused by hyperactive FGF signalling, we compared *Shh* expression between the various mutants and found that reducing *Fgfr1* gene dosage also rescued this defect in the sprouty mutants (Fig. 8E-G′). These observations suggest that a reduction in the availability of SHH ligand, in combination with the hypo-responsiveness of GCps to SHH, was responsible for the observed defects in GCp proliferation.

DISCUSSION

Since the initial demonstration that FGF8 is sufficient to mimic isthmic organiser activity in the mes/r1 region of the embryonic brain, a large body of work has accumulated to support an essential role for FGF signalling in the establishment, maintenance and patterning of r1 in the early embryo. In this paper, we show that the appropriate level of FGF signalling from the IsO is maintained by sprouty gene expression and that deregulated signalling in the absence of these genes affects normal growth and patterning. We show that all three sprouty genes expressed in the embryo are involved in this activity. In addition, we provide the first evidence for a continued role of these genes during later stages (post-E12.5) of cerebellar morphogenesis. Excessive FGF signalling in the absence of these genes affects the differentiation of multiple cell types and the proliferation of GCps.

Earlier studies on the role of FGF in the IsO have shown that high amounts of FGF8, ectopically applied on beads or via electroporation of *Fgf8*-expressing constructs, can transform the mes to r1 or induce mes expansion, depending on the strength of the FGF signal provided (Lee et al., 1997; Liu et al., 1999; Sato and Nakamura, 2004; Olsen et al., 2006). Overexpression of *Spry2* or dominant-negative *Spry2* in the chick mes/r1 inhibits or enhances FGF signalling resulting in mes/r1 fate changes (Suzuki-Hirano et al., 2005). By deleting endogenous antagonists in the mouse embryo we studied the consequences of increased FGF signalling in the context of normal expression (i.e. not ectopic) and found evidence for both a fate transformation early in development as well as an expansion of the mes later in development. Our observation of an expansion of the *Gbx2*-expressing anterior r1, apparently at the expense of *Otx2*-positive mes, is consistent with cell fate at the IsO being sensitive to the level of FGF signalling. However, we cannot rule out the possibility that a small increase in cell proliferation in anterior r1 might be the cause of this apparent change in gene expression. Furthermore, our observation that the posterior midbrain is expanded in sprouty mutant mice confirms previous observations showing that increased FGF signalling can also increase the size of the midbrain. The fact that the genetic manipulations we report here increase FGF signalling throughout cerebellar development might account for the fact that both an anterior expansion of r1 fate early in development (E9.5) and larger midbrain (by P0) are observed.

A number of previous studies have shown that the differentiation of cell types in the developing cerebellum are intimately linked. For example, Purkinje cell differentiation has been shown to require GCps (Berry and Bradley, 1976; Caddy and Herrup, 1990; Baptista et al., 1994). The regulation of GCp proliferation by PCs is well established (Lewis et al., 2004) and PC-derived signals control aspects of glial differentiation (Fukaya et al., 1999; Tam et al., 2010). In addition, the genetic ablation of glial cells has been shown to affect both PC differentiation and GCp proliferation (Delaney et al., 1996). Taking together our observations that BG express high amounts of sprouty transcripts (compared with the low or absent expression in other cell types) and that BG differentiation defects are present prior to GCp

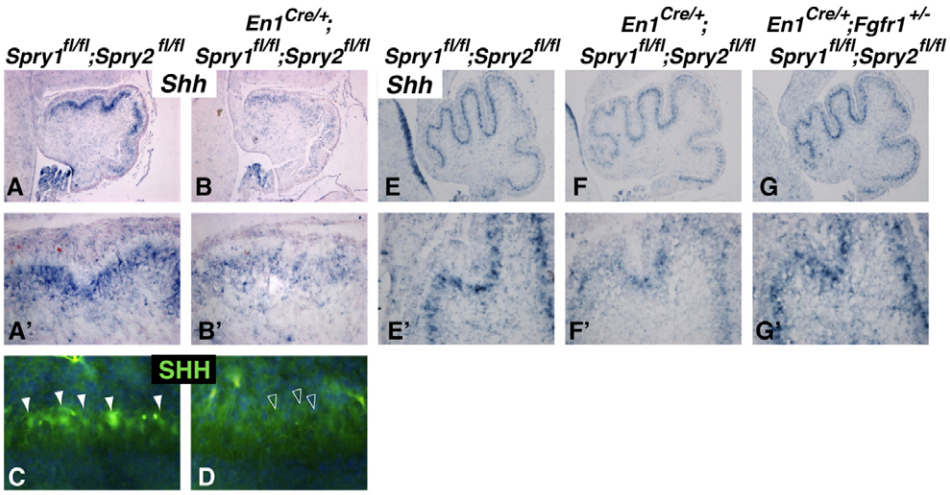

Fig. 8. SHH expression is reduced in sprouty-deficient cerebella. (**A-B′**) *Shh* expression was assayed on sagittal sections from E18.5 control (*Spry1*$^{fl/fl}$;*Spry2*$^{fl/fl}$) and mutant (*En1*$^{cre/+}$;*Spry1*$^{fl/fl}$;*Spry2*$^{fl/fl}$) mouse cerebella. A′ and B′ are high magnification views of A and B, respectively. (**C**,**D**) SHH protein distribution was determined by immunohistochemistry (green) on control and *En1*$^{cre/+}$;*Spry1*$^{fl/fl}$;*Spry2*$^{fl/fl}$ sections at P7, with nuclei counterstained with Hoechst (blue). White arrowheads in C indicate individual PCs with high levels of cytoplasmic SHH protein and open arrowheads in D indicate PCs with reduced SHH content. (**E-G′**) In situ hybridisation for *Shh* gene expression on sections from P0 control (E,E′), *En1*$^{cre/+}$;*Spry1*$^{fl/fl}$;*Spry2*$^{fl/fl}$ mutant (F,F′) and *En1*$^{cre/+}$;*Spry1*$^{fl/fl}$;*Spry2*$^{fl/fl}$;*Fgfr1*$^{+/-}$ rescue (G,G′) cerebella. E′, F′ and G′ are high magnification views of E, F and G, respectively.

proliferation defects becoming apparent, raises the possibility that these early glial defects might affect the development of several other cell types, including GCps. Interestingly, GCps have been shown to respond to at least one factor secreted by cerebellar astroglia, FGF2 (Hatten et al., 1988). As the deletion of sprouty genes in other developmental contexts are sometimes associated with increased FGF gene expression (Klein et al., 2008), we looked for changes in FGF gene expression in *En1*$^{cre/+}$;*Spry1*$^{flox/flox}$;*Spry2*$^{flox/flox}$ cerebella. However, no changes in *Fgf2*, *Fgf3*, *Fgf9* or *Fgf15* expression could be observed (data not shown). A recent study demonstrated that the deletion of FGF receptors during later stages of cerebellar development using *Nestin-Cre*, resulted in major cerebellar defects including GCp proliferation and migration defects (Lin et al., 2009). As the deletion of FGF receptor genes in GCps has little effect on development (Rob Wechsler-Reya, personal communication), the most likely explanation for the GCp defects in these conditional mutants is that they are secondary to early abnormalities in glial differentiation. It will be informative to delete FGF receptor and sprouty genes specifically in BG without affecting other cell types; unfortunately the availability of an appropriate Cre driver for simultaneous deletion of multiple conditional alleles remains a practical limitation.

Our study indicates that the maintenance of normal SHH signalling levels during cerebellar development requires sprouty gene function. We found that excess FGF signalling affected SHH signalling at more than one level: first, the expression of *Shh* is reduced in PCs and second, the level of SHH signalling is reduced in SHH-responsive cell types, including GCps. The latter observation is consistent with previous in vitro findings (Wechsler-Reya and Scott, 1999) but the effects on *Shh* expression has not previously been reported to our knowledge. The exact molecular mechanisms that underlie these effects remain to be determined and might have implications for other contexts in which SHH and FGF signalling are closely apposed (Kataoka and Shimogori, 2008).

In conclusion, we have found that several cell types in the developing cerebellum are sensitive to deregulated FGF signalling. Future experiments will be required to identify the individual roles of different FGF ligands and the exact interplay between different cerebellar cell types during development.

Acknowledgements
We thank Gail Martin, in whose laboratory this project was initiated, for her support, and several colleagues for providing mouse lines (Gill Bates, James Briscoe, Chuxia Deng, Alex Joyner, Gail Martin, David Ornitz, David Rowitch and Rob Wechsler-Reya) and in situ probes (Silvia Arber, Alex Joyner, Gail Martin). The 5E1 mAb developed by Tom Jessell was obtained from the Developmental Studies Hybridoma Bank developed under the auspices of the NICHD and maintained by The University of Iowa, Department of Biology, Iowa City, IA 52242. The PCP2 antiserum was a kind gift of Brad Denker (Harvard University). We thank Brian Emmenegger, Rob Wechsler-Reya, Gail Martin, Alex Joyner, Richard Wingate, Ivor Mason, Mary-Beth Hatten and Nadia Dahmane for valuable discussions, Clemens Kiecker and Philippa Francis-West for comments on the manuscript. Hagen Schmidt and Samantha Martin provided expert animal husbandry and technical support throughout the course of this project. This work was supported by grants from the Wellcome Trust to M.A.B. (080470 and 091475), the European commission (HEALTH-F4-2010-261492) and the Spanish MICINN (SAF2008-01004, BFU2008-00588 and CSD2007-00023) to D.E. and S.M. Deposited in PMC for release after 6 months.

Competing interests statement
The authors declare no competing financial interests.

Supplementary material
Supplementary material for this article is available at
http://dev.biologists.org/lookup/suppl/doi:10.1242/dev.063784/-/DC1

References
Baptista, C. A., Hatten, M. E., Blazeski, R. and Mason, C. A. (1994). Cell-cell interactions influence survival and differentiation of purified Purkinje cells in vitro. *Neuron* **12**, 243-260.
Basson, M. A., Akbulut, S., Watson-Johnson, J., Simon, R., Carroll, T. J., Shakya, R., Gross, I., Martin, G. R., Lufkin, T., McMahon, A. P. et al. (2005). Sprouty1 is a critical regulator of GDNF/RET-mediated kidney induction. *Dev. Cell* **8**, 229-239.
Basson, M. A., Echevarria, D., Ahn, C. P., Sudarov, A., Joyner, A. L., Mason, I. J., Martinez, S. and Martin, G. R. (2008). Specific regions within the

embryonic midbrain and cerebellum require different levels of FGF signaling during development. *Development* **135**, 889-898.
Berry, M. and Bradley, P. (1976). The growth of the dendritic trees of Purkinje cells in irradiated agranular cerebellar cortex. *Brain Res.* **116**, 361-387.
Bizzoca, A., Virgintino, D., Lorusso, L., Buttiglione, M., Yoshida, L., Polizzi, A., Tattoli, M., Cagiano, R., Rossi, F., Kozlov, S. et al. (2003). Transgenic mice expressing F3/contactin from the TAG-1 promoter exhibit developmentally regulated changes in the differentiation of cerebellar neurons. *Development* **130**, 29-43.
Bundschu, K., Walter, U. and Schuh, K. (2007). Getting a first clue about SPRED functions. *BioEssays* **29**, 897-907.
Caddy, K. W. and Herrup, K. (1990). Studies of the dendritic tree of wild-type cerebellar Purkinje cells in lurcher chimeric mice. *J. Comp. Neurol.* **297**, 121-131.
Chen, C., Ouyang, W., Grigura, V., Zhou, Q., Carnes, K., Lim, H., Zhao, G. Q., Arber, S., Kurpios, N., Murphy, T. L. et al. (2005). ERM is required for transcriptional control of the spermatogonial stem cell niche. *Nature* **436**, 1030-1034.
Chi, C. L., Martinez, S., Wurst, W. and Martin, G. R. (2003). The isthmic organizer signal FGF8 is required for cell survival in the prospective midbrain and cerebellum. *Development* **130**, 2633-2644.
Corrales, J. D., Rocco, G. L., Blaess, S., Guo, Q. and Joyner, A. L. (2004). Spatial pattern of sonic hedgehog signaling through Gli genes during cerebellum development. *Development* **131**, 5581-5590.
Corrales, J. D., Blaess, S., Mahoney, E. M. and Joyner, A. L. (2006). The level of sonic hedgehog signaling regulates the complexity of cerebellar foliation. *Development* **133**, 1811-1821.
Crossley, P. H., Martinez, S. and Martin, G. R. (1996). Midbrain development induced by FGF8 in the chick embryo. *Nature* **380**, 66-68.
Dahmane, N. and Ruiz i Altaba, A. (1999). Sonic hedgehog regulates the growth and patterning of the cerebellum. *Development* **126**, 3089-3100.
Delaney, C. L., Brenner, M. and Messing, A. (1996). Conditional ablation of cerebellar astrocytes in postnatal transgenic mice. *J. Neurosci.* **16**, 6908-6918.
Echevarria, D., Martinez, S., Marques, S., Lucas-Teixeira, V. and Belo, J. A. (2005). Mkp3 is a negative feedback modulator of Fgf8 signaling in the mammalian isthmic organizer. *Dev. Biol.* **277**, 114-128.
Fogarty, M. P., Emmenegger, B. A., Grasfeder, L. L., Oliver, T. G. and Wechsler-Reya, R. J. (2007). Fibroblast growth factor blocks Sonic hedgehog signaling in neuronal precursors and tumor cells. *Proc. Natl. Acad. Sci. USA* **104**, 2973-2978.
Fukaya, M., Yamada, K., Nagashima, M., Tanaka, K. and Watanabe, M. (1999). Down-regulated expression of glutamate transporter GLAST in Purkinje cell-associated astrocytes of reeler and weaver mutant cerebella. *Neurosci. Res.* **34**, 165-175.
Hatten, M. E. and Heintz, N. (1995). Mechanisms of neural patterning and specification in the developing cerebellum. *Annu. Rev. Neurosci.* **18**, 385-408.
Hatten, M. E., Liem, R. K. and Mason, C. A. (1984). Defects in specific associations between astroglia and neurons occur in microcultures of weaver mouse cerebellar cells. *J. Neurosci.* **4**, 1163-1172.
Hatten, M. E., Lynch, M., Rydel, R. E., Sanchez, J., Joseph-Silverstein, J., Moscatelli, D. and Rifkin, D. B. (1988). In vitro neurite extension by granule neurons is dependent upon astroglial-derived fibroblast growth factor. *Dev. Biol.* **125**, 280-289.
Herrup, K. and Kuemerle, B. (1997). The compartmentalization of the cerebellum. *Annu. Rev. Neurosci.* **20**, 61-90.
Hidalgo-Sanchez, M., Simeone, A. and Alvarado-Mallart, R. M. (1999). Fgf8 and Gbx2 induction concomitant with Otx2 repression is correlated with midbrain-hindbrain fate of caudal prosencephalon. *Development* **126**, 3191-3203.
Joyner, A. L., Liu, A. and Millet, S. (2000). Otx2, Gbx2 and Fgf8 interact to position and maintain a mid-hindbrain organizer. *Curr. Opin. Cell Biol.* **12**, 736-741.
Kataoka, A. and Shimogori, T. (2008). Fgf8 controls regional identity in the developing thalamus. *Development* **135**, 2873-2881.
Kenney, A. M., Cole, M. D. and Rowitch, D. H. (2003). Nmyc upregulation by sonic hedgehog signaling promotes proliferation in developing cerebellar granule neuron precursors. *Development* **130**, 15-28.
Kimmel, R. A., Turnbull, D. H., Blanquet, V., Wurst, W., Loomis, C. A. and Joyner, A. L. (2000). Two lineage boundaries coordinate vertebrate apical ectodermal ridge formation. *Genes Dev.* **14**, 1377-1389.
Klein, O. D., Minowada, G., Peterkova, R., Kangas, A., Yu, B. D., Lesot, H., Peterka, M., Jernvall, J. and Martin, G. R. (2006). Sprouty genes control diastema tooth development via bidirectional antagonism of epithelial-mesenchymal FGF signaling. *Dev. Cell* **11**, 181-190.
Klein, O. D., Lyons, D. B., Balooch, G., Marshall, G. W., Basson, M. A., Peterka, M., Boran, T., Peterkova, R. and Martin, G. R. (2008). An FGF signaling loop sustains the generation of differentiated progeny from stem cells in mouse incisors. *Development* **135**, 377-385.
Klein, R. S., Rubin, J. B., Gibson, H. D., DeHaan, E. N., Alvarez-Hernandez, X., Segal, R. A. and Luster, A. D. (2001). SDF-1 alpha induces chemotaxis and enhances Sonic hedgehog-induced proliferation of cerebellar granule cells. *Development* **128**, 1971-1981.
Lee, S. M., Danielian, P. S., Fritzsch, B. and McMahon, A. P. (1997). Evidence that FGF8 signalling from the midbrain-hindbrain junction regulates growth and polarity in the developing midbrain. *Development* **124**, 959-969.
Lewis, P. M., Gritli-Linde, A., Smeyne, R., Kottmann, A. and McMahon, A. P. (2004). Sonic hedgehog signaling is required for expansion of granule neuron precursors and patterning of the mouse cerebellum. *Dev. Biol.* **270**, 393-410.
Li, C., Scott, D. A., Hatch, E., Tian, X. and Mansour, S. L. (2007). Dusp6 (Mkp3) is a negative feedback regulator of FGF-stimulated ERK signaling during mouse development. *Development* **134**, 167-176.
Lin, W., Jing, N., Basson, M. A., Dierich, A., Licht, J. and Ang, S. L. (2005). Synergistic activity of Sef and Sprouty proteins in regulating the expression of Gbx2 in the mid-hindbrain region. *Genesis* **41**, 110-115.
Lin, Y., Chen, L., Lin, C., Luo, Y., Tsai, R. Y. and Wang, F. (2009). Neuron-derived FGF9 is essential for scaffold formation of Bergmann radial fibers and migration of granule neurons in the cerebellum. *Dev. Biol.* **329**, 44-54.
Liu, A., Losos, K. and Joyner, A. L. (1999). FGF8 can activate Gbx2 and transform regions of the rostral mouse brain into a hindbrain fate. *Development* **126**, 4827-4838.
Liu, A., Li, J. Y., Bromleigh, C., Lao, Z., Niswander, L. A. and Joyner, A. L. (2003). FGF17b and FGF18 have different midbrain regulatory properties from FGF8b or activated FGF receptors. *Development* **130**, 6175-6185.
Machold, R. and Fishell, G. (2005). Math1 is expressed in temporally discrete pools of cerebellar rhombic-lip neural progenitors. *Neuron* **48**, 17-24.
Mahoney Rogers, A. A., Zhang, J. and Shim, K. (2011). Sprouty1 and Sprouty2 limit both the size of the otic placode and hindbrain Wnt8a by antagonizing FGF signaling. *Dev. Biol.* **353**, 94-104.
Martinez, S., Crossley, P. H., Cobos, I., Rubenstein, J. L. and Martin, G. R. (1999). FGF8 induces formation of an ectopic isthmic organizer and isthmocerebellar development via a repressive effect on Otx2 expression. *Development* **126**, 1189-1200.
Martynoga, B., Morrison, H., Price, D. J. and Mason, J. O. (2005). Foxg1 is required for specification of ventral telencephalon and region-specific regulation of dorsal telencephalic precursor proliferation and apoptosis. *Dev. Biol.* **283**, 113-127.
Mason, J. M., Morrison, D. J., Basson, M. A. and Licht, J. D. (2006). Sprouty proteins: multifaceted negative-feedback regulators of receptor tyrosine kinase signaling. *Trends Cell Biol.* **16**, 45-54.
Matei, V., Pauley, S., Kaing, S., Rowitch, D., Beisel, K. W., Morris, K., Feng, F., Jones, K., Lee, J. and Fritzsch, B. (2005). Smaller inner ear sensory epithelia in Neurog 1 null mice are related to earlier hair cell cycle exit. *Dev. Dyn.* **234**, 633-650.
Minowada, G., Jarvis, L. A., Chi, C. L., Neubuser, A., Sun, X., Hacohen, N., Krasnow, M. A. and Martin, G. R. (1999). Vertebrate Sprouty genes are induced by FGF signaling and can cause chondrodysplasia when overexpressed. *Development* **126**, 4465-4475.
Miyazawa, K., Himi, T., Garcia, V., Yamagishi, H., Sato, S. and Ishizaki, Y. (2000). A role for p27/Kip1 in the control of cerebellar granule cell precursor proliferation. *J. Neurosci.* **20**, 5756-5763.
Nakamura, H., Sato, T. and Suzuki-Hirano, A. (2008). Isthmus organizer for mesencephalon and metencephalon. *Dev. Growth Differ.* **50 Suppl. 1**, S113-S118.
Olsen, S. K., Li, J. Y., Bromleigh, C., Eliseenkova, A. V., Ibrahimi, O. A., Lao, Z., Zhang, F., Linhardt, R. J., Joyner, A. L. and Mohammadi, M. (2006). Structural basis by which alternative splicing modulates the organizer activity of FGF8 in the brain. *Genes Dev.* **20**, 185-198.
Partanen, J. (2007). FGF signalling pathways in development of the midbrain and anterior hindbrain. *J. Neurochem.* **101**, 1185-1193.
Sato, T. and Nakamura, H. (2004). The Fgf8 signal causes cerebellar differentiation by activating the Ras-ERK signaling pathway. *Development* **131**, 4275-4285.
Sato, T. and Joyner, A. L. (2009). The duration of Fgf8 isthmic organizer expression is key to patterning different tectal-isthmo-cerebellum structures. *Development* **136**, 3617-3626.
Schimmang, T., Lemaistre, M., Vortkamp, A. and Ruther, U. (1992). Expression of the zinc finger gene Gli3 is affected in the morphogenetic mouse mutant extra-toes (Xt). *Development* **116**, 799-804.
Schuller, U., Zhao, Q., Godinho, S. A., Heine, V. M., Medema, R. H., Pellman, D. and Rowitch, D. H. (2007). Forkhead transcription factor FoxM1 regulates mitotic entry and prevents spindle defects in cerebellar granule neuron precursors. *Mol. Cell. Biol.* **27**, 8259-8270.
Sgaier, S. K., Millet, S., Villanueva, M. P., Berenshteyn, F., Song, C. and Joyner, A. L. (2005). Morphogenetic and cellular movements that shape the mouse cerebellum; insights from genetic fate mapping. *Neuron* **45**, 27-40.
Shim, K., Minowada, G., Coling, D. E. and Martin, G. R. (2005). Sprouty2, a mouse deafness gene, regulates cell fate decisions in the auditory sensory epithelium by antagonizing FGF signaling. *Dev. Cell* **8**, 553-564.

Sillitoe, R. V. and Joyner, A. L. (2007). Morphology, molecular codes, and circuitry produce the three-dimensional complexity of the cerebellum. *Annu. Rev. Cell Dev. Biol.* **23**, 549-577.
Simeone, A., Acampora, D., Mallamaci, A., Stornaiuolo, A., D'Apice, M. R., Nigro, V. and Boncinelli, E. (1993). A vertebrate gene related to orthodenticle contains a homeodomain of the bicoid class and demarcates anterior neuroectoderm in the gastrulating mouse embryo. *EMBO J.* **12**, 2735-2747.
Solecki, D. J., Liu, X. L., Tomoda, T., Fang, Y. and Hatten, M. E. (2001). Activated Notch2 signaling inhibits differentiation of cerebellar granule neuron precursors by maintaining proliferation. *Neuron* **31**, 557-568.
Sotelo, C. (2004). Cellular and genetic regulation of the development of the cerebellar system. *Prog. Neurobiol.* **72**, 295-339.
Sotelo, C. and Changeux, J. P. (1974). Bergmann fibers and granular cell migration in the cerebellum of homozygous weaver mutant mouse. *Brain Res.* **77**, 484-491.
Suzuki-Hirano, A., Sato, T. and Nakamura, H. (2005). Regulation of isthmic Fgf8 signal by sprouty2. *Development* **132**, 257-265.
Takahashi, T., Nowakowski, R. S. and Caviness, V. S., Jr (1993). Cell cycle parameters and patterns of nuclear movement in the neocortical proliferative zone of the fetal mouse. *J. Neurosci.* **13**, 820-833.
Takahashi, T., Nowakowski, R. S. and Caviness, V. S., Jr (1996). The leaving or Q fraction of the murine cerebral proliferative epithelium: a general model of neocortical neuronogenesis. *J. Neurosci.* **16**, 6183-6196.
Tam, W. Y., Leung, C. K., Tong, K. K. and Kwan, K. M. (2010). Foxp4 is essential in maintenance of PURKINJE cell dendritic arborization in the mouse cerebellum. *Neuroscience* **172**, 562-571.
Taniguchi, K., Ayada, T., Ichiyama, K., Kohno, R., Yonemitsu, Y., Minami, Y., Kikuchi, A., Maehara, Y. and Yoshimura, A. (2007). Sprouty2 and Sprouty4 are essential for embryonic morphogenesis and regulation of FGF signaling. *Biochem. Biophys. Res. Commun.* **352**, 896-902.
Trokovic, R., Trokovic, N., Hernesniemi, S., Pirvola, U., Vogt Weisenhorn, D. M., Rossant, J., McMahon, A. P., Wurst, W. and Partanen, J. (2003). FGFR1 is independently required in both developing mid- and hindbrain for sustained response to isthmic signals. *EMBO J.* **22**, 1811-1823.
Tronche, F., Kellendonk, C., Kretz, O., Gass, P., Anlag, K., Orban, P. C., Bock, R., Klein, R. and Schutz, G. (1999). Disruption of the glucocorticoid receptor gene in the nervous system results in reduced anxiety. *Nat. Genet.* **23**, 99-103.
Wallace, V. A. (1999). Purkinje-cell-derived Sonic hedgehog regulates granule neuron precursor cell proliferation in the developing mouse cerebellum. *Curr. Biol.* **9**, 445-448.
Wang, B., Fallon, J. F. and Beachy, P. A. (2000). Hedgehog-regulated processing of Gli3 produces an anterior/posterior repressor gradient in the developing vertebrate limb. *Cell* **100**, 423-434.
Wassarman, K. M., Lewandoski, M., Campbell, K., Joyner, A. L., Rubenstein, J. L., Martinez, S. and Martin, G. R. (1997). Specification of the anterior hindbrain and establishment of a normal mid/hindbrain organizer is dependent on Gbx2 gene function. *Development* **124**, 2923-2934.
Wechsler-Reya, R. J. and Scott, M. P. (1999). Control of neuronal precursor proliferation in the cerebellum by Sonic Hedgehog. *Neuron* **22**, 103-114.
Wilkinson, D. G., Bhatt, S., Cook, M., Boncinelli, E. and Krumlauf, R. (1989a). Segmental expression of Hox-2 homoeobox-containing genes in the developing mouse hindbrain. *Nature* **341**, 405-409.
Wilkinson, D. G., Bhatt, S. and McMahon, A. P. (1989b). Expression pattern of the FGF-related proto-oncogene int-2 suggests multiple roles in fetal development. *Development* **105**, 131-136.
Wingate, R. J. (2001). The rhombic lip and early cerebellar development. *Curr. Opin. Neurobiol.* **11**, 82-88.
Xu, X., Qiao, W., Li, C. and Deng, C. X. (2002). Generation of Fgfr1 conditional knockout mice. *Genesis* **32**, 85-86.
Yacubova, E. and Komuro, H. (2003). Cellular and molecular mechanisms of cerebellar granule cell migration. *Cell Biochem. Biophys.* **37**, 213-234.
Yaguchi, Y., Yu, T., Ahmed, M. U., Berry, M., Mason, I. and Basson, M. A. (2009). Fibroblast growth factor (FGF) gene expression in the developing cerebellum suggests multiple roles for FGF signaling during cerebellar morphogenesis and development. *Dev. Dyn.* **238**, 2058-2072.
Zervas, M., Blaess, S. and Joyner, A. L. (2005). Classical embryological studies and modern genetic analysis of midbrain and cerebellum development. *Curr. Top. Dev. Biol.* **69**, 101-138.
Zhang, X., Ibrahimi, O. A., Olsen, S. K., Umemori, H., Mohammadi, M. and Ornitz, D. M. (2006). Receptor specificity of the fibroblast growth factor family. The complete mammalian FGF family. *J. Biol. Chem.* **281**, 15694-15700.

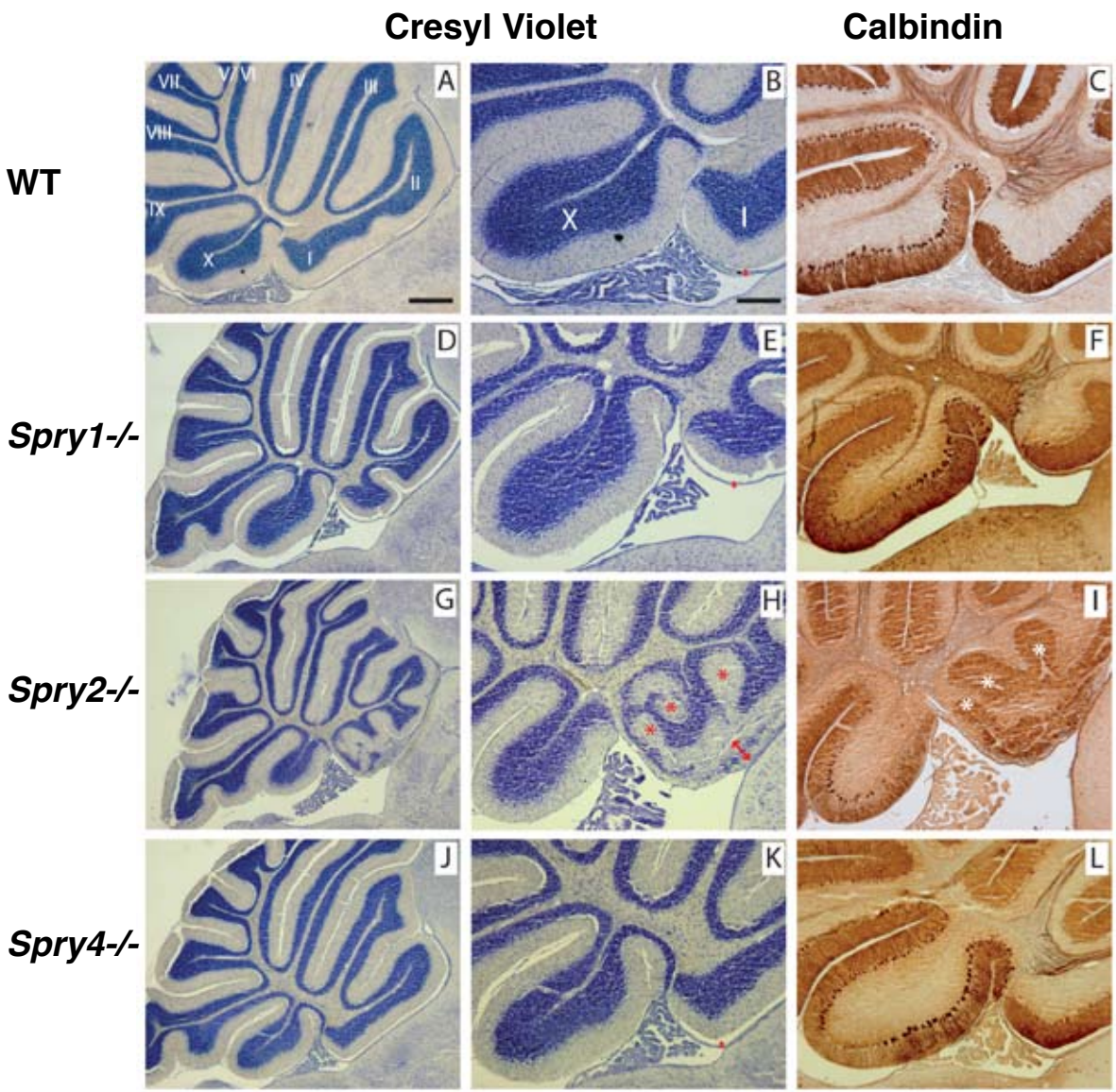
Cresyl Violet
Calbindin
WT
Spry1-/-
Spry2-/-
Spry4-/-
A
B
C
D
E
F
G
H
I
J
K
L
VII
V/VI
IV
III
VIII
II
IX
X
I

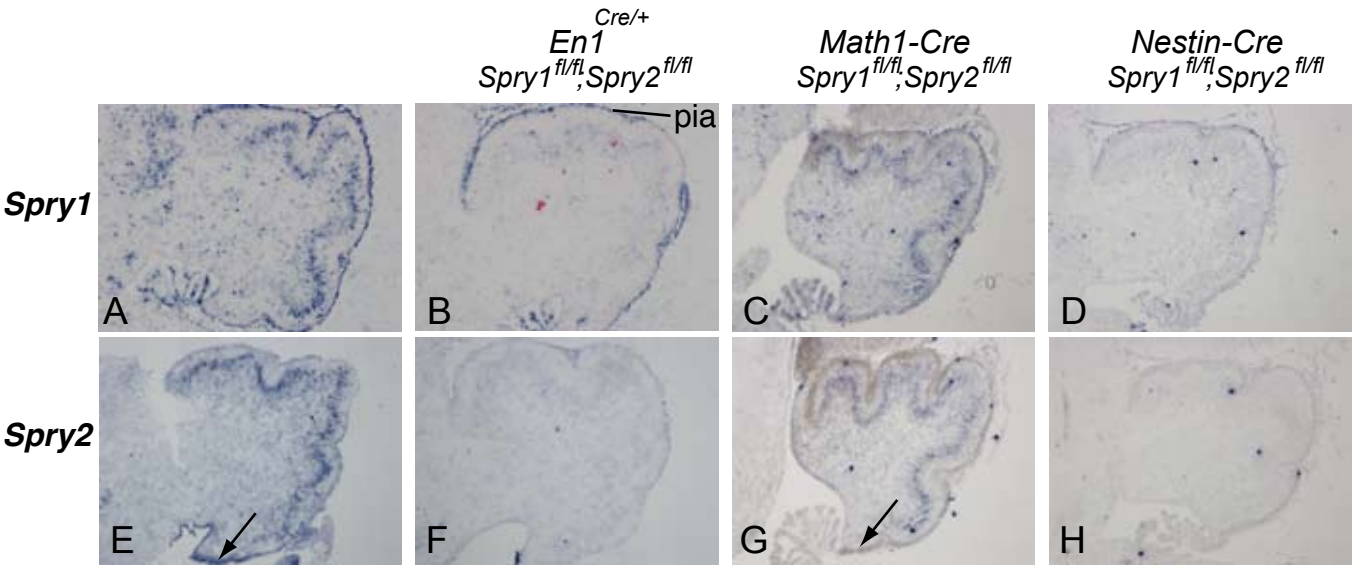
En1 Cre/+
Spry1fl/fl;Spry2fl/fl
Math1-Cre
Spry1fl/fl;Spry2fl/fl
Nestin-Cre
Spry1fl/fl;Spry2fl/fl
Spry1
Spry2
pia
A
B
C
D
E
F
G
H

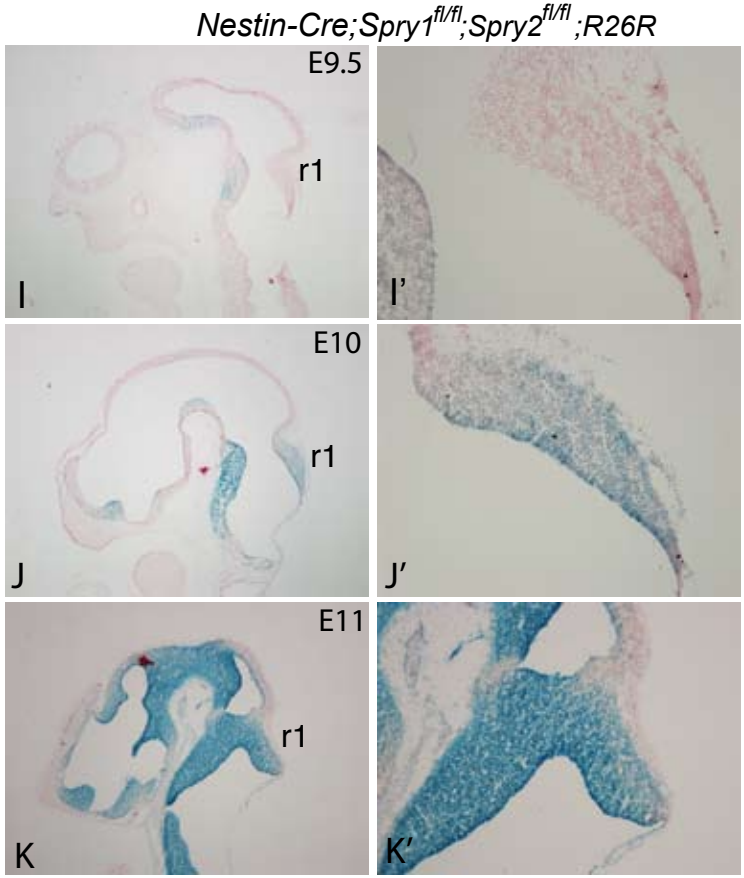
Nestin-Cre;Spry1fl/fl;Spry2fl/fl;R26R
E9.5
r1
I
I'
E10
r1
J
J'
E11
r1
K
K'

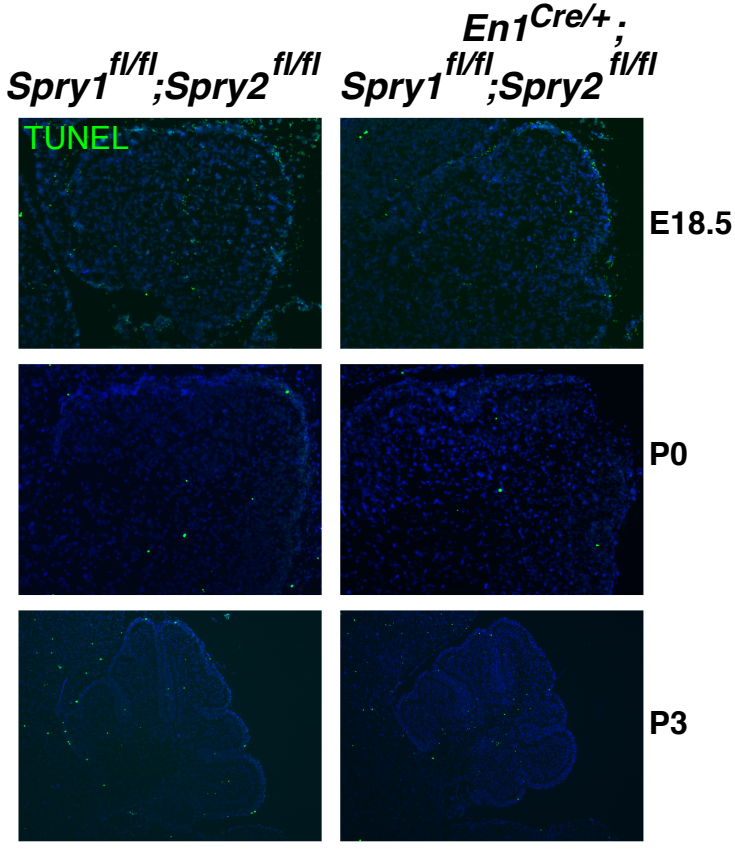
Spry1fl/fl;Spry2fl/fl
En1Cre/+; Spry1fl/fl;Spry2fl/fl
TUNEL
E18.5
P0
P3